Multicarrier Spread Spectrum for Covert Acoustic Communications

Paul van Walree
TNO, Underwater Technology Group
Oude Waalsdorperweg 63
2509 JG The Hague, The Netherlands
E-mail: paul.vanwalree@tno.nl

Erland Sangfelt
Swedish Defence Research Agency FOI
SE-164 90
Stockholm, Sweden
E-mail: erland.sangfelt@foi.se

Geert Leus
Delft University of Technology
Mekelweg 4
2628 CD Delft, The Netherlands
E-mail: g.j.t.leus@tudelft.nl

***Abstract*— A multicarrier modulation scheme is presented to achieve the objective of clandestine acoustic communications. The modulation consists of a single bit sequence simultaneously modulated onto multiple carriers. As all bands carry the same symbol stream, they can be adaptively combined with a multichannel equalizer. A multiband equalizer with K feedforward filters is thus devised for joint equalization and despreading of K frequency bands. The idea is tested on acoustic data collected during sea experiments in the Baltic Sea. Eight carriers were used to divide the available bandwidth up into $K = 8$ binary phase-shift keyed bands of 460 Hz each. Covert operation at low SNR is enabled by the spread-spectrum gain delivered by the adaptive combiner, a rate-1/3 turbo coding scheme, and through the use of periodic training. Results are shown for three experiments over ranges of 8, 28, and 52 km, using a prototype acoustic modem as the transmitter and a hydrophone at the receiving end. Both the modem and the hydrophone were lowered into the Baltic sound channel from surface ships. At an effective data rate of 75 bit/s, the user message is correctly recovered at SNRs down to –12 dB under various multipath conditions. A comparison is made with two other modulations, direct-sequence spread spectrum and orthogonal frequency-division multiplexing. These signals were broadcast during the same experiments, in the same frequency band, and at the same data rate. The proposed multicarrier scheme compares favorably with the other modulations.**

I. Introduction

The joint European research project "UUV Covert Acoustic Communications" (UCAC) explores methods for furtive acoustic communications in littoral environments. Wireless datalinks are to be established between a mother ship and an unmanned underwater vehicle (UUV) over ranges up to 50 km. The primary objectives are 1) convey the message correctly and 2) covertness in the sense of a low probability of detection by third parties. The challenge in UCAC is to hide waveforms in the ambient noise by conveying the user message at as low as possible an SNR. In order to achieve this, spread-spectrum techniques are applied, together with powerful error correcting codes. Several modulations are explored in the UCAC project. From the start of the project three candidates have been considered: direct-sequence spread-spectrum (DSSS, [1]), orthogonal frequency-division multiplexing (OFDM, [2]), and a chirp-based modulation [3]. The present paper describes a fourth modulation, termed multicarrier spread spectrum (MCSS), which was added before the second UCAC sea trial in 2007. This modulation protects the user message through channel coding, repetition coding, and periodic training. The repetition coding is applied in the frequency domain and is adaptively decoded by a multichannel equalizer.

Multichannel equalizers have been developed in the context of space-time signal processing [4], [5], exploiting diverse signal signatures received on spatially separated antennas. The spatial dimension allows a level of signal enhancement and interference cancellation that cannot be achieved with single-receiver systems. However, applicability of multichannel receivers is not restricted to spatially separated receivers. The present paper applies multichannel equalization to a single hydrophone, equalizing parallel frequency bands which carry identical symbol sequences. Existing MCSS work was presented in [6] and [7], but without the adaptive equalization and combining required for many underwater channels. The key operation principle of the proposed MCSS receiver is a multiband equalizer which performs joint equalization and despreading of the frequency bands. Other features are periodic training, a reduced-complexity recursive least-quares (RLS) equalizer update algorithm, and an iterative adaptive turbo approach which runs in different forward and backward passes.

This paper is organized as follows. Section II and III describe the MCSS transmitter and receiver structure, respectively. Section IV gives some pertinent facts about the UCAC sea trial and characteristics of the acoustic channel. Section V presents MCSS results for these channels and also compares the MCSS method with DSSS and OFDM. The paper is concluded in Section VI.

Notation: Upper case bold face letters represent matrices, lower case bold face letters column vectors; $(\cdot)^T$ denotes nonconjugate transpose and $(\cdot)^*$ conjugate. $\Re(x)$ denotes the real part of x and $\mathrm{E}(\cdot)$ stands for the expectation; $\mathbf{0}_N$ denotes a column vector with N zeros and $\mathbf{I}_{N\times N}$ the $N \times N$ identity matrix.

II. Transmitter

A. Constraints

The modulations explored within the UCAC project have to meet a few conditions. First, all waveforms should use a common bandwidth of $\mathcal{B} = 3.5$ kHz. This constraint

978-1-4244-2620-1/08/$25.00 ©2008 IEEE

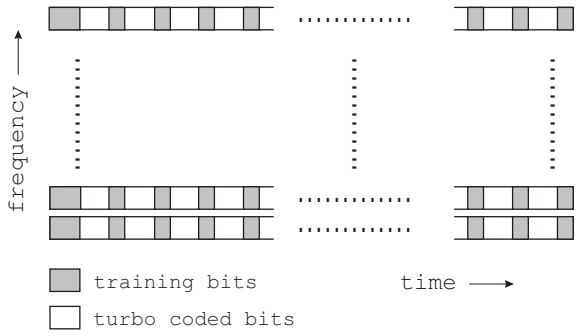

Fig. 1. Schematic depiction of the multicarrier modulation.

basically follows from the transfer function of the transmitter, a prototype acoustic modem. The adopted bandwidth criterion is that at least 95% of the energy of the supplied waveforms is confined to a 3.5-kHz band. Second, two target information data rates were specified at 4.2 and 75 bps for messages of 125 and 1911 user bits, respectively. A margin of a few percent is allowed in the rates, as too tight a tolerance may adversely affect performance. The bit rates are the effective rates, taking into account all overhead. Both messages are rate-1/3 turbo encoded bit streams, to be used for all modulations. Thus the bandwidth, user message and number of bits, channel coder and decoder, and signal duration (through the specified data rate) are common parameters. Otherwise there is complete freedom to design transmitters and receivers. The DSSS, OFDM, and Chirp schemes were prepared for transmission at 4.2 and 75 bps. The MCSS modulation was a last-minute addition, and was prepared only at 75 bps.

B. MCSS Modulation

Fig. 1 depicts the modulation, whereas the main elements of the transmitter are shown schematically in the left part of Fig. 2. The transmitted waveform uses $N = 8767$ binary phase-shift keyed symbols $z(n) \in \{-1, 1\}$, comprising 127 bits for detection and equalizer convergence, 2880 periodic training bits, and 5760 turbo coded bits. A maximal-length sequence is used for the 127-bit preamble, and a standard parallel turbo encoder [8] is used for the channel coding. The interleaver internal to the turbo decoder has a length of 640 bits [9] and encodes 637 information bits, as the three tail bits are reserved to terminate the first constituent encoder. Three code blocks are used, adding up to 1911 user bits. The coded bits and training bits are interleaved in 45 packets with 64 training bits and 128 code bits. The resulting symbol stream $\mathbf{z} = [z(1), ..., z(N)]^T$ is simultaneously modulated onto K carriers to obtain the transmit waveform

$$s(t) = \sum_{k=1}^{K} \sum_{n=1}^{N} z(n) p(t - nT) \exp\left(\mathrm{i}\omega_k t\right) , \qquad (1)$$

where ω_k gives the angular carrier frequency of the k-th subband. T denotes the symbol duration, with $T^{-1} = 345\ \mathrm{s}^{-1}$ the symbol rate. A raised-cosine spectrum [10] is adopted for the elementary pulse $p(t)$, using a roll-off factor $\beta = 1/3$. Its spectrum covers a total frequency band of $B = (1 + \beta)/T = 460$ Hz. $K = 8$ of such bands are combined in a single waveform with a 100%-energy bandwidth of $KB = 3680$ Hz. The carriers are connected to the overall center frequency by

$$\omega_k = \omega_\mathrm{c} + 2\pi \left(k - \frac{K+1}{2}\right) B \ . \qquad (2)$$

Guard bands are omitted as the smooth raised-cosine spectral roll-off provides sufficient protection against interband interference. The carrier frequency amounts to $f_\mathrm{c} = \omega_\mathrm{c}/2\pi = 3300$ Hz.

III. Receiver

The receiver operations consist of an acquisition phase; an adaptive-filter phase which implements joint equalization, despreading and phase tracking; bit estimation; application of a turbo decoder. Soft information from the turbo decoder is subsequently used to repeat the equalization phase with enhanced channel tracking capability. A more detailed description of what follows is provided in [11].

A. Acquisition

The received data $\tilde{u}(t)$ are brought to complex baseband with respect to the overall center frequency

$$u(t) = \tilde{u}(t) \exp(-\mathrm{i}\omega_\mathrm{c} t) \ , \qquad (3)$$

and correlated with a bank of Doppler-shifted replicas of the detection part of the signal. For improved detection, 128 coded bits are "borrowed" and combined with the original 127-bit sequence to yield an effective 255-symbol detection preamble. Since the signal is wideband, the Doppler shifts are performed through resampling. This resampling is indicated by the operator D_v, with v the relative TX/RX velocity, and with the resampling applied relative to a nominal sound speed of 1500 m/s. A filter bank is used with 101 Doppler replicas running from -4 to $+4$ m/s in 8-cm/s steps. Recorded data are fed to the correlator in rms-normalized blocks of several seconds. The peak correlator output is obtained across all Doppler channels, and if its value exceeds a certain threshold a signal is considered acquired with a corresponding Doppler velocity v_det and signal start t_det. The estimated Doppler shift and timing offset are removed and the constituent frequency bands are separately basebanded

$$u_k(t) = D_{-v_\mathrm{det}} \left[u(t - t_\mathrm{det})\right] \exp[-\mathrm{i}(\omega_k - \omega_\mathrm{c})t] \qquad (4)$$

for $k = 1, ..., K$. Notice that the signal is thus synchronized on the strongest multipath arrival in the correlator filter output. A brick-wall bandpass filter is used to remove energy outside each frequency band, followed by an overall rms normalization

$$y_k(t) = u_k(t) \left(\frac{1}{KNT} \sum_{k=1}^{K} \int_0^{NT} u_k(t) u_k^*(t) \, \mathrm{d}t \right)^{-1/2} . \qquad (5)$$

The sole purpose of the normalization is to speed up equalizer convergence by presenting samples whose magnitude is approximately known, which enables an appropriate choice for the initial condition of the adaptive filter.

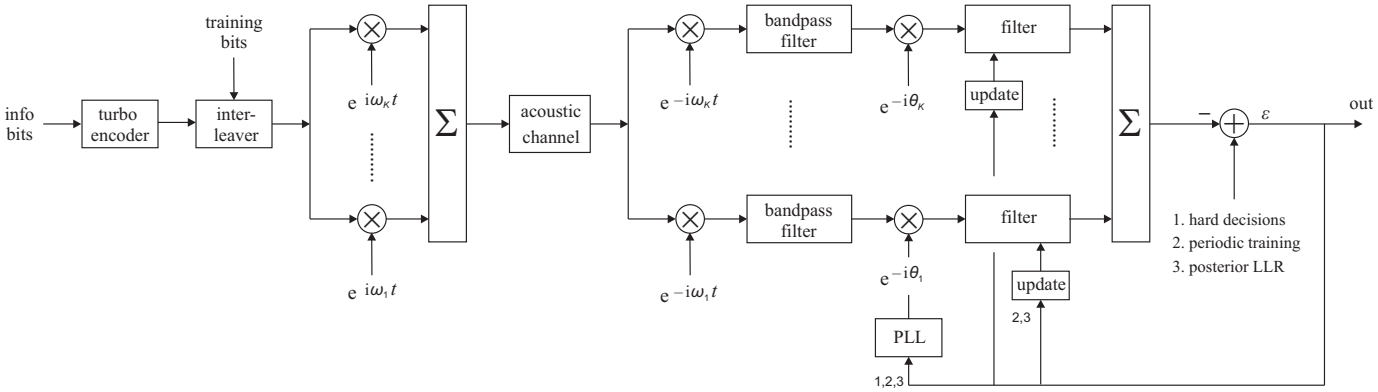

Fig. 2. Block diagram of the transmitter and receiver, separated by the channel.

B. Adaptive Filtering

Basic elements of the equalizer structure are depicted in the right half of Fig. 2. The baseband signals $y_k(t)$ are downsampled to 4 samples per symbol, phase shifted via a phase-locked loop (PLL) as indicated in the figure, and fed to a fractionally-spaced ($3T/4$) multichannel equalizer with $L = 14$ taps per frequency channel. The equalization process is initialized with the strongest peak of the correlation detector output centered in the feedforward filters. To obtain the n-th symbol estimate, each band is separately equalized and the results are summed

$$\hat{z}(n) = \sum_{k=1}^{K} \mathbf{y}_{k,n}^T \, \mathbf{c}_{k,n-1} \ , \tag{6}$$

where $\mathbf{c}_{k,n-1}$ is the previous equalizer for the k-th carrier. An integrated PLL [5] is also used to mitigate residual phase drifts that remain after elimination of the estimated mean Doppler shift. The PLL is tuned to the overall center frequency and yields an estimate of the phase offset $\theta(n)$. Phase compensation is applied to each sub-band separately according to $\theta_k(n) = (\omega_k/\omega_c) \times \theta(n)$. A single error signal is computed as

$$\varepsilon(n) = z_{\mathrm{ref}}(n) - \hat{z}(n) \ , \tag{7}$$

where $z_{\mathrm{ref}}(n)$ is a reference symbol selected according to several criteria (see Section III-C). The equalizers $\mathbf{c}_{k,n}$ are updated using a separate RLS scheme for each frequency band, guided by the common error signal $\varepsilon(n)$. The Kalman gain vector $\mathbf{g}_{k,n}$, filter coefficients $\mathbf{c}_{k,n}$, and $\mathbf{P}_{k,n}$ (the inverse correlation matrix) are updated as

$$\mathbf{g}_{k,n} = \frac{\mathbf{P}_{k,n-1}\mathbf{y}_{k,n}^*}{\lambda + \sum_{k'=1}^{K} \mathbf{y}_{k',n}^T \mathbf{P}_{k',n-1} \mathbf{y}_{k',n}^*} \ , \tag{8}$$

$$\mathbf{c}_{k,n} = \mathbf{c}_{k,n-1} + \mathbf{g}_{k,n} \, \varepsilon(n) \ , \tag{9}$$

$$\mathbf{P}_{k,n} = \lambda^{-1} \left[\mathbf{P}_{k,n-1} - \mathbf{g}_{k,n} \mathbf{y}_{k,n}^T \mathbf{P}_{k,n-1} \right] \ , \tag{10}$$

using a forgetting factor $\lambda = 0.999$. The adaptive filter is initialized with $\mathbf{c}_{k,0} = \mathbf{0}_L$ and $\mathbf{P}_{k,0} = \mathbf{I}_{L\times L}$, which is an appropriate initialization of the inverse correlation matrix considering the normalization (5) of the received signal.

The update equations (8)–(10) are derived from a single standard RLS update [10], where all frequency bands are combined in a single vector $\mathbf{y}_n = [\mathbf{y}_{1,n}^T, \ldots, \mathbf{y}_{K,n}^T]^T$, by assuming that all cross-correlations between frequency bands are negligible. Note in this regard that the coherence bandwidth is of order T_{delay}^{-1}, where T_{delay} is the delay spread of the channel. Characteristic delay spreads of underwater acoustic channels lead to a frequency coherence much smaller than the sub-band separation of 460 Hz. As a result the frequency channels are mutually uncorrelated, and there is no need for a joint RLS update which allows for cross-correlations. The advantage is a reduction in computation time equal to the number of frequency bands. If all bands are combined in a single vector, the computational complexity of the RLS tap update is $\mathcal{O}(K^2L^2)$, which equals the complexity of a chip-level DSSS equalizer covering the same time-delay span and overall frequency band. Separate RLS updates, on the other hand, reduce the complexity to $\mathcal{O}(KL^2)$.

C. Iterations

Initially the quantities (8)–(10) are only updated during the designated training periods, and frozen in between. Following equalization of the entire signal, probabilities are computed for the equalized symbols to represent a zero or a one. These probabilities are obtained with the help of the known periodic training symbols, on the assumption that their real parts are described by normal distributions. See [11] for more details. A prior log-likelihood ratio (LLR) is computed and fed to a standard turbo decoder [8]. The decoder returns a posterior LLR, from which a probability is extracted of bits being zero or one after the decoder. This probability is subsequently used to perform a second equalization sweep, which runs in reversed time. The adaptive filter equalizes from the last symbol back to the first, starting with coefficients that already converged during the first equalization stage. Moreover, taps are not only updated during the allocated training periods, but also when the probability of a bit being zero or one exceeds a threshold $\Gamma = 0.9$. The corresponding symbols are thus

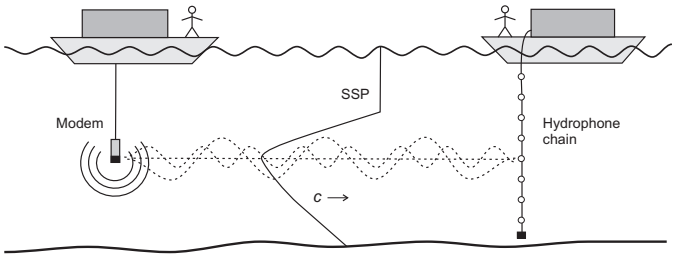

Fig. 3. Depiction of the Baltic sea trial. The figure also sketches the sound speed profile (SSP) and a few rays trapped in the sound channel.

added as additional training symbols with a high probability of being correct. In this manner the equalizer operates back and forth, improving the BER in cases with a slow initial convergence and more generally through an increase of the tap update rate. The PLL is updated without interruptions, using hard decisions on the equalized symbols if nothing better is available.

IV. UCAC Sea Trial 2007

A. Sea Trial

Sea experiments were performed in northern Europe, in August 2007. Experiments from the Baltic Sea are considered, where the covert UCAC waveforms were broadcast with a prototype acoustic modem. The area was just east of the Danish island Bornholm [12]. At a water depth of 70 m, measured sound speed profiles reveal a local minimum at a depth of about 40 m. The sound channel thus created acts as an acoustic waveguide, and allows long-range signaling. Fig. 3 shows the setup. The modem was suspended in the sound channel, at a depth of 40 m, through the moon pool of a surface ship (Fig. 4). This ship used dynamic positioning to remain at a given location during communication experiments. A vertical hydrophone chain was deployed from another, anchored ship. A single element is employed for the analysis, located within

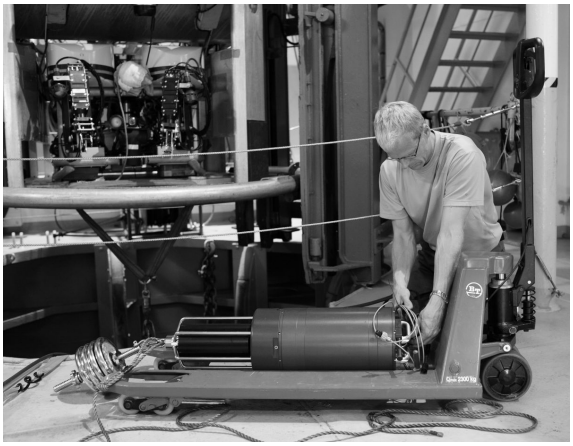

Fig. 4. The UCAC acoustic modem is prepared for deployment through the moon pool visible in the background.

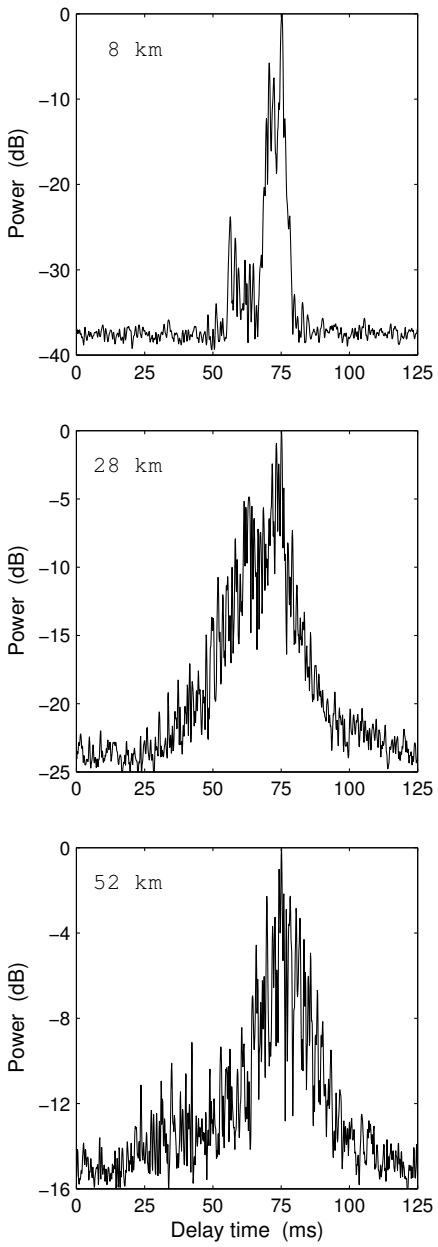

Fig. 5. Characteristic power delay profiles for the three examined ranges. The profiles are obtained with the probe signal, using the method described in [13].

the sound channel at a depth of 50 m. Three distances between the two ships are examined in the analysis: 8, 28, and 52 km. Impulse responses measured in the Baltic sound channel display a crescendo of multipath arrivals, followed by a decay on a shorter time scale. Measured power delay profiles are shown in Fig. 5. With the transmitter and receiver depths fixed, the range is the primary variable. A dense pattern of multipath arrivals is observed, with a delay spread that increases with range. The coherence time of these channels is several tens of seconds, but there is some Doppler in the form of relative TX/RX motion which requires phase tracking.

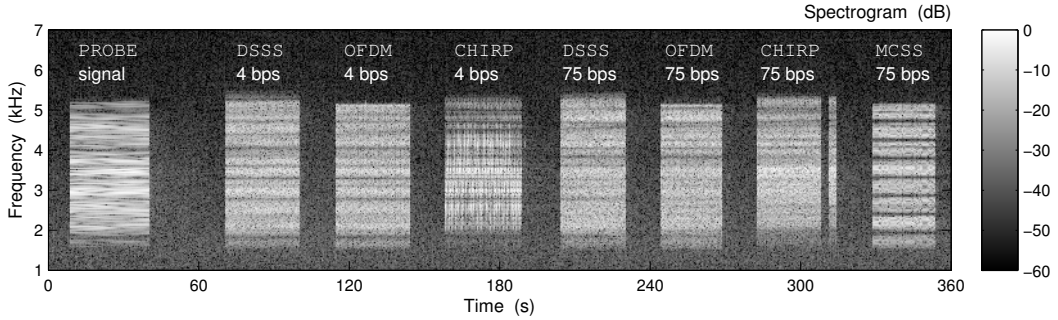

Fig. 6. Full cycle with eight waveforms (8-km range, SNR $\approx +24$ dB).

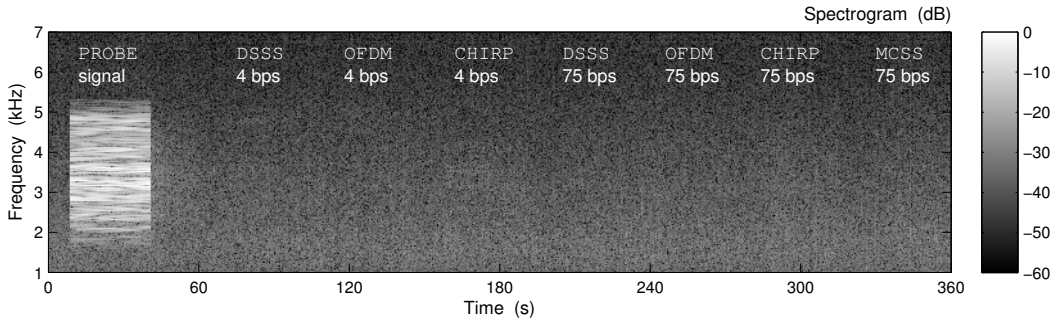

Fig. 7. Full cycle with eight waveforms (8-km range, SNR ≈ -12 dB).

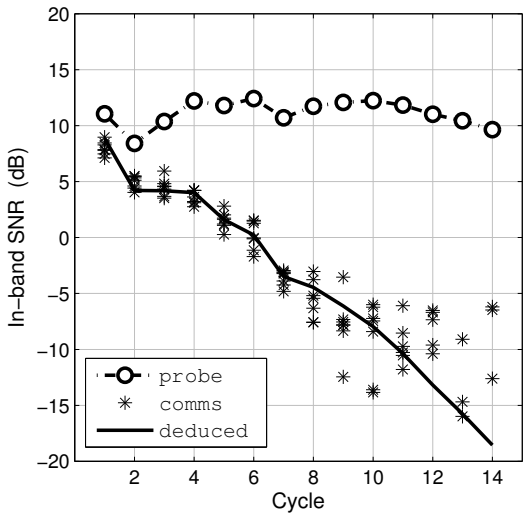

Fig. 8. SNR computation illustrated for the 28-km range.

B. SNR Computation

The MCSS signal was part of a periodic broadcast schedule. A 360-s transmit wavefile was constructed with eight signals, one probe signal and seven "covert" communication signals. The probe signal, the pseudorandom binary sequence described in [13], was placed at the start of the waveform. The wavefile was repeatedly broadcast, and with each cycle the source level of all signals except the probe was reduced by 2 dB. The seven communication waveforms are rms-equalized, i.e., within a given cycle they have the same rms level at the transmitter. Fig. 6 shows the first of a succession of twenty of such cycles, received at a high SNR of $+24$ dB. By contrast, Fig. 7 shows the eighteenth cycle, received at an estimated SNR of -12 dB. These SNRs are measured by comparison of received signal-plus-noise energy in the frequency band of the signals, with the energy of noise alone. An ideal bandpass filter is applied to the baseband data $u(t)$

$$w(t) = \mathcal{B} \int \operatorname{sinc}\big(\mathcal{B}(t-\tau)\big) u(\tau)\, \mathrm{d}\tau \ . \tag{11}$$

The in-band signal $w(t)$ is subsequently used to estimate an SNR according to

$$\mathrm{SNR} = \frac{\displaystyle\int_{\mathcal{T}_1} |w(t)|^2\, \mathrm{d}t \left(\int_{\mathcal{T}_1} \mathrm{d}t \right)^{-1}}{\displaystyle\int_{\mathcal{T}_2} |w(t)|^2\, \mathrm{d}t \left(\int_{\mathcal{T}_2} \mathrm{d}t \right)^{-1}} - 1 \ , \tag{12}$$

where $\mathcal{T}_1$ denotes a period known to contain signal and noise, and $\mathcal{T}_2$ covers several periods known to contain only noise. At low values of the SNR, long integration intervals are required to obtain reliable estimates. Eight sections of four seconds are adopted for $\mathcal{T}_2$, preceding the eight waveforms depicted in Fig. 6. Notice in this regard that the arrival times of the covert waveforms are approximately known, also at low SNR such as in Fig. 7, from the overt probe signal at the start of each cycle. The integrals in the denominator of (12) thus run over a total of 32 seconds, and sparsely average noise over the duration of

TABLE I

BIT ERROR RATIOS AT 8 KM. A DASH INDICATES A DETECTION FAILURE.

SNR (dB)	DSSS	OFDM	DSSS	OFDM	MCSS
	4.2 bps	4.2 bps	75 bps	75 bps	75 bps
$+1.1$	0	0	0	0	0
-0.7	0	0	0	0	0
-2.1	0	0	0	0	0
-4.9	0	0	0	0	0
-6.1	0	0	0	0	0
-8.5	0	0	0	0	0
-9.2	0	0	0	0	0
-12.1	0	0	0.341	0.228	0
-13.9	0	0	—	0.288	0.157
-16.5	0	0	—	0.416	0.208

TABLE II

BIT ERROR RATIOS AT 28 KM. A DASH INDICATES A DETECTION FAILURE.

SNR (dB)	DSSS	OFDM	DSSS	OFDM	MCSS
	4.2 bps	4.2 bps	75 bps	75 bps	75 bps
$+1.6$	0	0	0	0	0
$+0.2$	0	0	0	0	0
-3.5	0	0	0	0	0
-4.5	0	0	0.108	0	0
-6.1	0	0	0.038	0	0
-8.0	0	0	0.331	0.023	0
-10.4	0	0	0.417	0.128	0
-13.2	—	0	—	0.395	0.200
-15.8	—	—	—	0.365	—
-18.5	—	—	—	—	—

TABLE III

BIT ERROR RATIOS AT 52 KM. A DASH INDICATES A DETECTION FAILURE.

SNR (dB)	DSSS	OFDM	DSSS	OFDM	MCSS
	4.2 bps	4.2 bps	75 bps	75 bps	75 bps
$+0.6$	0	0	0	0	0
-1.9	0	0	0	0	0
-4.3	0	0	0	0	0
-6.5	0	0	0	0	0
-8.5	0	0	0.506	0	0
-9.2	0	0	—	0.060	0
-12.7	0	0	—	0.183	0
-14.4	0	0	—	0.331	0
-17.6	—	—	—	—	—
-19.2	—	—	—	—	—

a cycle. For $\mathcal{T}_1$ one could select data portions within the covert waveforms, but this yields an unreliable estimate at very low SNR. Instead, a portion is selected within the probe signal. The known relationship between the source levels of the probe and communication waveforms is used to deduce the SNR of the latter.

Fig. 8 exemplifies this procedure for the 28-km signaling range. The round markers give the SNR that results when $\mathcal{T}_1$ is chosen to represent a 20-s portion of the received probe signals. Asterisks give the SNRs for $\mathcal{T}_1$ representing 20-s portions of received communication waveforms. There are seven of these per cycle, but as the SNR decreases their values become increasingly unreliable or negative even. The thick black curve is deduced from the probe signal SNR and is the leading estimate at low values. Its fidelity can be judged at high SNR, where the asterisks are close to this curve. The scatter or uncertainty is about 2 dB, and is caused by the time variations of signal and noise levels.

V. RESULTS

A. MCSS Performance

Three sea experiments are evaluated in terms of the bit error ratio (BER). The modem was used to broadcast the periodic scheme described in the previous section, over the channels whose power delay profiles are shown in Fig. 5. The MCSS receiver is fully automated and works its way through recorded data with a fixed set of parameters. Although up to twenty cycles were transmitted and recorded, Tables I, II, and III only list ten cycles in the interesting regime of low SNR. The SNR in these tables is estimated with the help of the overt probe signal, as discussed in Section IV-B. Considering the uncertainty of ≈ 2 dB in the SNR estimates, one finds that error-free MCSS reception is possible down to an SNR of ≈ -12 dB, regardless of the delay spread.

The benefit of the iterative equalization scheme is demonstrated by Figs. 9 and 10, which illustrate the receiver operation for the sixth signal of Table III, received at an SNR of about -10 dB. Fig. 9 shows a receiver diagnostics screen after a single equalization pass. The top-left panel shows the correlator output for a 10-s interval, including detection at 6 s. The power spectral density in the top-right panel is averaged over the duration of the signal and just bears evidence of a few frequency bands between 3 and 5 kHz. At lower frequencies the signal energy is overpowered by the colored noise. The mean square error $\mathrm{E}\left(|\varepsilon(n)|^2\right)$, and the phase estimate $\theta(n)$ are shown in the middle panels. The bottom panels display the equalized symbols $\hat{z}(n)$ and a histogram of their real parts. Thick black curves represent the normal distributions used for the computation of the prior LLR [11]. The shape of these curves is obtained from the periodic training, and their amplitude is scaled to obtain the same total area under curves and bars.

The situation for three equalization sweeps, one forward, one backward, and another forward one, is shown in Fig. 10. This figure omits the detection and spectrum panels, which have not changed. An overall improvement is noticed for the MSE, especially during the first thousand or so symbols, as the equalizer has already adapted to the channel when it commences the final forward pass. The residual phase is nearly identical to that of the first pass, which suggests that the iteration gain is mostly achieved by better adaptation of the equalizer coefficients. The constellation clouds are better separated, although this is easier to tell from the histogram

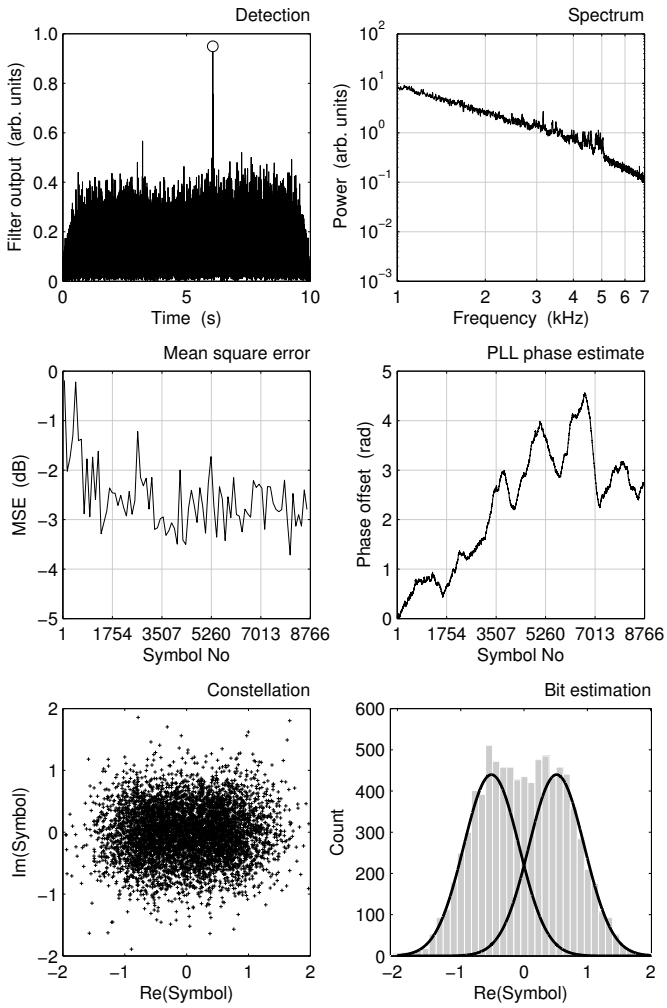

Fig. 9. MCSS receiver diagnostics for an example reception over 52 km, an estimated SNR of ≈ -10 dB, and a single equalization pass.

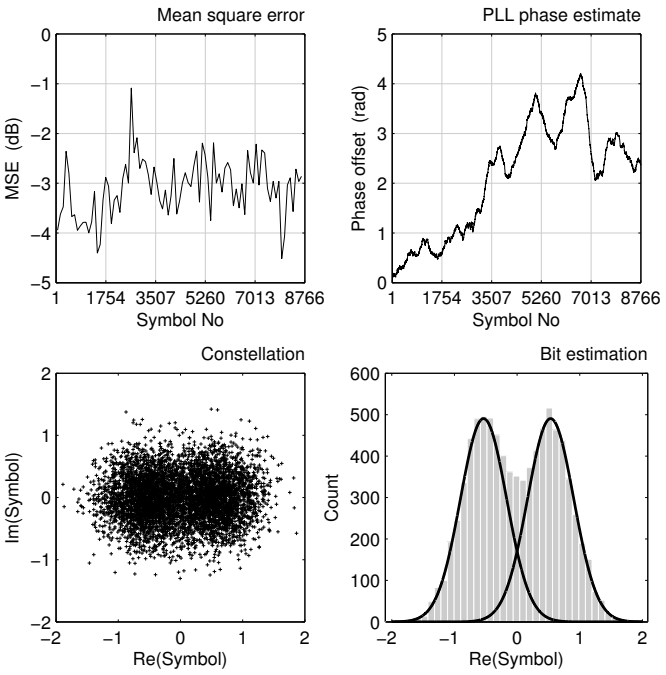

Fig. 10. Bottom four panels of Fig. 9, but after three equalization stages.

than from the clouds themselves. Notice that the two clouds are not centered on ± 1, but that they are closer to the origin. This shift is a well-known property of Wiener filters operating at low SNR.

B. Comparison with DSSS and OFDM

Tables I–III compare the MCSS performance with that of a DSSS [1] scheme employing turbo equalization and a multi-band OFDM scheme [2]. A comparison with the chirp-based method described in [3] is difficult because this paper gives the uncoded BER, whereas Tables I–III present the coded BER. The BER of DSSS and OFDM is given given at both UCAC data rates. It is emphasized that the numbers in the tables, or any other conclusion drawn in this section, do not necessarily point to fundamental differences between modulations. Even if different groups would explore the same modulation, it is unlikely that the results would be the same, since transmitters and receiver strategies, and specific implementations can differ.

Although the statistics are poor at one reception per signal per cycle, with an uncertainty of ≈ 2 dB in the SNRs, the BERs in Tables I–III reveal several interesting trends. At 4.2 bit/s the BER for DSSS and OFDM is either zero or undefined (failure of detection). At 8 km, the lowest achieved SNR is not low enough to observe the transition, but the situation is clear at 28 and 52 km. All communication schemes use noiselike, Doppler-sensitive detection preambles with a duration of order 1 s. In all cases detection is performed by correlating data with a bank of Doppler-shifted preamble replicas, and comparing the correlator output with a threshold. In the presence of multipath propagation, or Doppler effects, the detection performance at a given SNR drops. Long delay spreads require long preambles, but the longer the preamble the more sensitive it becomes to Doppler variations during its transmission. Currently the performance at 4.2 bps is limited by detection; the limits of the communication receivers themselves are not exposed.

Although detection failures also occur at 75 bps, they do not limit the performance at this data rate. BERs between zero and 50% indicate proper detection and synchronization, but failure of the communication receivers to deliver the message correctly. At 8 km, DSSS and OFDM offer a comparable performance. MCSS does a little better and recovers the message for one more cycle. The advantage of MCSS increases with range. At 52 km it decodes three or four cycles more than the competition, which corresponds to an SNR advantage of 6–8 dB. The only known difference between the three channels, apart from the range, is the corresponding delay spread. MCSS appears to be robust with respect to the increasing delay spread, whereas DSSS and OFDM appear to be more vulnerable. Quite remarkably, at 52 km, MCSS

performs as well at 75 bps as DSSS and OFDM at 4.2 bps. Of course, the potential for stealth data transfer is much higher at 4.2 bps, and DSSS and OFDM might go down further in SNR if it were not for the detection problem.

The eighth entry of Table I is shown in Fig. 7. At an estimated SNR of -12 dB, it is almost impossible to find evidence of the communication waveforms. They are inaudible upon playing the sound, and only observers who know what to look for may find visual clues. Nonetheless, from this cycle the 4.2-bps DSSS and OFDM receptions, and the 75-bps MCSS reception can be demodulated. Note that DSSS and OFDM are still successful when the SNR has decreased by a further 4 dB, at which point all signals except the probe are completely invisible and inaudible.

As stressed before the results do not directly qualify one modulation as being more suitable than another for covert communications. For example, the DSSS scheme lacks a dedicated phase-tracking loop, which is an important element of the MCSS receiver. OFDM, on the other hand, does not employ iterative turbo equalization, which is an ingredient of the DSSS and MCSS receivers. Thus ideas exist to further improve the DSSS and OFDM schemes. Although the SNR performance determines the capability to hide the communication link from energy detectors, other qualities are important too. Aurally, from all the UCAC waveforms DSSS is the most noiselike. At a given SNR, these signals are least likely to be noticed by eavesdropping sonar operators. OFDM performs a little worse, which is due to a specific structure of pilot carriers and repetition coding that can be discerned by the ear. MCSS is the worst performer in this regard and has a raspy sound due to the repetition of identical bands in the frequency domain. The receivers for both OFDM and MCSS have a short demodulation time, unlike DSSS. On the other hand, DSSS has a lower crest factor than both multicarrier schemes and can be transmitted at higher source levels if a long range is requested. Several criteria were used in the UCAC project to evaluate the candidate covert modulations, and all candidates have strong and weak points.

VI. Concluding Remarks

A multicarrier spread-spectrum modulation is presented for acoustic communication at low SNR. Its main principle of operation is joint equalization and despreading of contiguous frequency bands which carry the same symbol stream. The proposed MCSS scheme is compared with other candidate modulations, all tested during the same sea trial under the same conditions. With the current implementations of the various receivers, a comparison of the SNR performance at 75 bps is in favor of MCSS and its adaptive multiband turbo equalization scheme. Robust operation is demonstrated at SNRs down to -12 dB with an automated receiver and fixed parameters, for channels with different delay spreads. Application of MCSS to a more dynamic channel [11] still yields an SNR limit of ≈ -12 dB. Communication at still lower SNRs can be achieved by reducing the MCSS data rate. There are several ways to achieve this, but at any rate special attention should be paid to the detection problem, which proved to be the limiting factor for the 4.2-bps DSSS and OFDM rates.

Acknowledgment

The work described in this publication was done under a multinational, three-year project aimed at developing and demonstrating long-range covert acoustic communication with unmanned underwater vehicles (UUVs) in coastal waters. This project under the EUROPA MOU ERG No1 is known under the name RTP 110.060 "UUV Covert Acoustic Communications". The project partners are: Kongsberg Maritime AS (Norway); Fincantieri (Italy); Reson A/S (Denmark); TNO Defence, Security and Safety (Netherlands); Patria Systems (Finland); and Saab Underwater Systems AB (Sweden). The Federal Armed Forces Underwater Acoustics and Marine Geophysics Research Institute (FWG) has been commissioned by the Federal Office of Defence Technology and Procurement (BWB) (Germany). Subcontractors are the national defence research establishments of Sweden (FOI) and Norway (FFI), Cetena (Italy), the University of Genova (also Italy), and Delft University of Technology (the Netherlands).

References

[1] E. Sangfelt, B. Nilsson, and J. Israelsson, "Covert underwater communication experiments using DSSS and turbo equalization," in *UDT Europe 2008*, Glasgow, United Kingdom, June 2008.

[2] G. Leus, P. van Walree, J. Boschma, C. Fanciullacci, J. Gerritsen, and P. Tusoni, "Covert underwater communications with OFDM," in *OCEANS 2008*, Quebec City, Canada, September 2008.

[3] M. Palmese, G. Bertolotto, A. Pescetto, and A. Trucco, "Experimental validation of a chirp-based underwater acoustic communication method," in *Acoustics '08*, Paris, France, July 2008.

[4] A. J. Paulraj and C. B. Papadias, "Space-time processing for wireless communications," *IEEE Signal Process. Mag.*, vol. 14, no. 6, pp. 49–83, November 1997.

[5] M. Stojanovic, J. Catipovic, and J. G. Proakis, "Adaptive multichannel combining and equalization for underwater acoustic communications," *J. Acoust. Soc. Am.*, vol. 94, no. 3, pp. 1621–1631, September 1993.

[6] N. Yee, J. P. Linnartz, and G. Fettweis, "Multi-carrier CDMA in indoor wireless radio," in *IEEE PIMRC '93*, Yokohama, Japan, September 1993, pp. 109–113.

[7] K. Frazel and L. Papke, "On the performance of convolutionally-coded CDMA/OFDM for mobile communication system," in *IEEE PIMRC '93*, Yokohama, Japan, September 1993, pp. 468–472.

[8] C. Heegard and S. B. Wicker, *Turbo Coding*, Springer, 1998.

[9] Johan Hokfelt, "Interleaver download," http://www.tde.lth.se/home/jht/interleaverdownload.html, 2001.

[10] J. G. Proakis, *Digital Communications*, McGraw-Hill, fourth edition, 2001.

[11] P. A. van Walree and G. Leus, "Robust underwater telemetry with adaptive turbo multiband equalization," *IEEE J. Oceanic. Eng.*, 2008, submitted.

[12] H. S. Dol, F. Gerdes, P. A. van Walree, W. Jans, and S. Künzel, "Acoustic channel characterization in the Baltic Sea and in the North Sea," in *OCEANS 2008*, Quebec City, Canada, September 2008.

[13] P. A. van Walree, T. Jenserud, and M. Smedsrud, "A discrete-time channel simulator driven by measured scattering functions," *IEEE J. Sel. Areas Commun.*, 2008, submitted.